DETERMINATION OF V_{cb} AND V_{ub}

Updated February 2012 by R. Kowalewski (Univ. of Victoria, Canada) and T. Mannel (Univ. of Siegen, Germany)

INTRODUCTION

Precision determinations of $|V_{ub}|$ and $|V_{cb}|$ are central to testing the CKM sector of the Standard Model, and complement the measurements of CP asymmetries in B decays. The length of the side of the unitarity triangle opposite the well-measured angle β is proportional to the ratio $|V_{ub}|/|V_{cb}|$, making its determination a high priority of the heavy-flavor physics program.

The semileptonic transitions $b \to c\ell\overline{\nu}_\ell$ and $b \to u\ell\overline{\nu}_\ell$ provide two avenues for determining these CKM matrix elements, namely through inclusive and exclusive final states. The experimental and theoretical techniques underlying these two avenues are independent, providing a crucial cross-check on our understanding. Recent measurements and calculations are reflected in the values quoted in this article, which is an update on the previous review [1]. The leptonic decay $B^- \to \tau\overline{\nu}$ can also be used to extract $|V_{ub}|$, but we do not use this information at present since none of the current experimental measurements have a significance above 3.6σ.

The theory underlying the determination of $|V_{qb}|$ is mature, in particular for $|V_{cb}|$. Most of the theoretical approaches use the fact that the mass m_b of the b quark is large compared to the scale $\Lambda_{\rm QCD}$ that determines low-energy hadronic physics. The basis for precise calculations is a systematic expansion in powers of Λ/m_b, where $\Lambda \sim 500 - 700$ MeV is a hadronic scale of the order of $\Lambda_{\rm QCD}$, using effective-field-theory methods to separate non-perturbative from perturbative contributions. The expansion in Λ/m_b and α_s works well enough to enable a precision determination of $|V_{cb}|$ and $|V_{ub}|$ in semileptonic decays.

The large data samples available at the B factories enable analyses where one B meson from an $\Upsilon(4S)$ decay is fully reconstructed, allowing a recoiling semileptonic B decay to be studied with high purity. Improved knowledge of $\overline{B} \to X_c\ell\overline{\nu}_\ell$ decays allows partial rates for $\overline{B} \to X_u\ell\overline{\nu}_\ell$ transitions to be

measured in regions previously considered inaccessible, increasing the acceptance for $\overline{B} \to X_u \ell \overline{\nu}_\ell$ transitions and reducing theoretical uncertainties.

Experimental measurements of the exclusive $\overline{B} \to \pi \ell \overline{\nu}_\ell$ decay are quite precise, and recent improvements in the theoretical calculation of the form factor normalization have enabled a determination of $|V_{ub}|$ from this decay with an uncertainty below 10%.

Throughout this review the numerical results quoted are based on the methods of the Heavy Flavor Averaging Group [2].

DETERMINATION OF $|V_{cb}|$

Summary: The determination of $|V_{cb}|$ from $\overline{B} \to D^* \ell \overline{\nu}_\ell$ decays is currently at a relative precision of about 2%. The main limitation is the knowledge of the form factor near the maximum momentum transfer to the leptons. For the $\overline{B} \to D \ell \overline{\nu}_\ell$ channel experimental measurements have recently been substantially improved, allowing this channel to provide a meaningful cross-check on $\overline{B} \to D^* \ell \overline{\nu}_\ell$.

Determinations of $|V_{cb}|$ from inclusive decays are currently below 2% relative uncertainty. The limitations arise mainly from our ignorance of higher-order perturbative and non-perturbative corrections.

The values obtained from inclusive and exclusive determinations are marginally consistent with each other:

$$|V_{cb}| = (41.9 \pm 0.7) \times 10^{-3} \text{ (inclusive)} \quad (1)$$

$$|V_{cb}| = (39.6 \pm 0.9) \times 10^{-3} \text{ (exclusive)}. \quad (2)$$

An average of the above gives $|V_{cb}| = (40.9 \pm 0.6) \times 10^{-3}$, with $p(\chi^2) = 0.04$. Scaling the error by $\sqrt{\chi^2/1} = 2.0$ we quote

$$|V_{cb}| = (40.9 \pm 1.1) \times 10^{-3} \ . \quad (3)$$

$|V_{cb}|$ from exclusive decays

Exclusive determinations of $|V_{cb}|$ are based on a study of semileptonic B decays into the ground state charmed mesons D and D^*. The main uncertainties in this approach stem from our ignorance of the form factors describing the $B \to D$ and

$B \to D^*$ transitions. However, in the limit of infinite bottom and charm quark masses only a single form factor appears, the Isgur-Wise function [3], which depends on the product of the four-velocities v and v' of the initial and final-state hadrons.

The extraction of $|V_{cb}|$ is based on the distribution of the variable $w \equiv v \cdot v'$, which corresponds to the energy of the final state $D^{(*)}$ meson in the rest frame of the decay. Heavy Quark Symmetry (HQS) [3,4] predicts the normalization of the rate at $w = 1$, the point of maximum momentum transfer to the leptons, and $|V_{cb}|$ is obtained from an extrapolation of the measured spectrum to $w = 1$. This extrapolation relies on a parametrization of the form factor, as explained below.

A precise determination requires corrections to the HQS prediction for the normalization as well as some information on the slope of the form factors near the point $w = 1$, since the phase space vanishes there. The corrections to the HQS prediction due to finite quark masses are given in terms of the symmetry-breaking parameter

$$\frac{1}{\mu} = \frac{1}{m_c} - \frac{1}{m_b} ,$$

which is essentially $1/m_c$ for realistic quark masses. HQS ensures that those matrix elements that correspond to the currents that generate the HQS are normalized at $w = 1$; as a result, some of the form factors either vanish or are normalized to unity at $w = 1$. Due to Luke's Theorem [5] (which is an application of the Ademollo-Gatto theorem [6] to heavy quarks), the leading correction to those form factors normalized due to HQS is quadratic in $1/\mu$, while for the form factors that vanish in the infinite mass limit the corrections are in general linear in $1/m_c$ and $1/m_b$. Thus we have, using the definitions as in Eq. (2.84) of Ref. [7]

$$\begin{aligned} h_i(1) &= 1 + \mathcal{O}(1/\mu^2) \qquad \text{for } i = +, V, A_1, A_3 \ , \\ h_i(1) &= \mathcal{O}(1/m_c,\, 1/m_b) \qquad \text{for } i = -, A_2 \ . \end{aligned} \tag{4}$$

In addition to these corrections, there are perturbatively calculable radiative corrections from QCD and QED, which will be discussed in the relevant sections. Both - radiative

corrections as well as $1/m_{b,c}$ corrections - are considered in the framework of Heavy Quark Effective Theory (HQET) [8], which provides for a systematic expansion.

$\overline{B} \to D^* \ell \overline{\nu}_\ell$

The decay rate for $\overline{B} \to D^* \ell \overline{\nu}_\ell$ is given by

$$\frac{d\Gamma}{dw}(\overline{B} \to D^* \ell \overline{\nu}_\ell) = \frac{G_F^2}{48\pi^3} |V_{cb}|^2 m_{D^*}^3 (w^2-1)^{1/2} P(w) (\eta_{\rm em} \mathcal{F}(w))^2, \tag{5}$$

where $P(w)$ is a phase space factor with $P(1) = 12(m_B - m_{D^*})^2$ and $\mathcal{F}(w)$ is dominated by the axial vector form factor h_{A_1} as $w \to 1$. Furthermore, $\eta_{\rm em} = 1.007$ accounts for the electroweak corrections to the four-fermion operator mediating the semileptonic decay [11]. In the infinite-mass limit, the HQS normalization gives $\mathcal{F}(1) = 1$.

The form factor $\mathcal{F}(w)$ must be parametrized to perform an extrapolation to the zero-recoil point. A frequently used one-parameter form motivated by analyticity and unitarity is [9,10]

$$\mathcal{F}(w) = \eta_{\rm A} \left[1 + \delta_{1/m^2} + \cdots\right] \left[1 - 8\rho_{\rm A1}^2 z + (53\rho_{\rm A1}^2 - 15) z^2 - (231\rho_{\rm A1}^2 - 91) z^3\right] \tag{6}$$

with $z = (\sqrt{w+1} - \sqrt{2})/(\sqrt{w+1} + \sqrt{2})$ originating from a conformal transformation. The parameter $\rho_{\rm A1}^2$ is the slope of the form factor at $w = 1$. The factor $\eta_{\rm A}$ is the QCD short-distance radiative correction [12] to the form factor

$$\eta_{\rm A} = 0.960 \pm 0.007, \tag{7}$$

and δ_{1/m^2} comes from non-perturbative $1/m^2$ corrections.

Improved lattice simulations that include effects from finite quark masses are used to calculate the deviation of $\mathcal{F}(1)$ from unity. A recent calculation gives

$$\mathcal{F}(1) = 0.902 \pm 0.017, \tag{8}$$

where the factor $\eta_{\rm em}$ has been divided out from the value quoted in Ref. [13] and the errors have been added in quadrature. The leading uncertainties are due to heavy-quark discretization and chiral extrapolation errors.

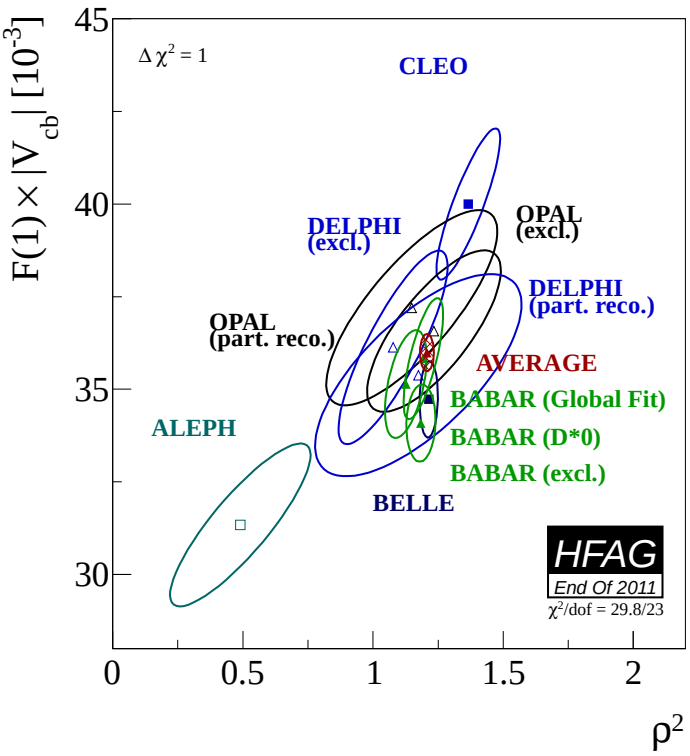

Figure 1: Measurements of $|V_{cb}|\mathcal{F}(1)$ vs. $\rho^2_{A_1}$ are shown as $\Delta\chi^2 = 1$ ellipses.

Non-lattice estimates based on sum rules for the form factor tend to yield lower values for $\mathcal{F}(1)$ [14,15,16]. Omitting the contributions from excited states, the sum rules indicate that $\mathcal{F}(1) < 0.93$. Including an estimate for the contribution of the excited states yields $\mathcal{F}(1) = 0.86 \pm 0.01 \pm 0.02$ [16]. where the second uncertainty originates from the estimate for the excited states.

Many experiments [17–25] have measured the differential rate as a function of w. Fig. 1 shows corresponding values of $\mathcal{F}(1)\,|V_{cb}|$ and $\rho^2_{A_1}$ (as defined in Ref. [10]) . These measurements are input to a four-dimensional fit [26] for $\mathcal{F}(1)|V_{cb}|$, $\rho^2_{A_1}$ and the form factor ratios $R_1 \propto A_2/A_1$ and $R_2 \propto V/A_1$. The leading sources of uncertainty on $\mathcal{F}(1)\,|V_{cb}|$ are due to detection efficiencies and $D^{(*)}$ decay branching fractions, while for $\rho^2_{A_1}$ the uncertainties in R_1 and R_2 still dominate. Recent BABAR measurements, one using $\overline{B}^0 \to D^{*0}\ell\overline{\nu}_\ell$ decays [23] and the

other using a global fit to $\overline{B} \to D\ell\overline{\nu}_\ell X$ decays [24] are completely insensitive to uncertainties related to the reconstruction of the charged pion from $D^* \to D\pi$ decays; both measurements agree with the average given below.

The fit gives $\mathcal{F}(1)\,|V_{cb}| = (36.0 \pm 0.5) \times 10^{-3}$ with a p-value of 0.15. Along with the lattice value given above for $\mathcal{F}(1)$ this yields

$$|V_{cb}| = (39.6 \pm 0.6_{\rm exp} \pm 0.8_{\rm theo}) \times 10^{-3} \quad (\overline{B} \to D^*\ell\overline{\nu}_\ell,\ \text{LQCD}). \tag{9}$$

The value of $\mathcal{F}(1)$ obtained from QCD sum rules results in a larger value for $|V_{cb}|$:

$$|V_{cb}| = (41.6 \pm 0.6_{\rm exp} \pm 1.9_{\rm theo}) \times 10^{-3} \quad (\overline{B} \to D^*\ell\overline{\nu}_\ell,\ \text{SR}). \tag{10}$$

$\overline{B} \to D\ell\overline{\nu}_\ell$

The differential rate for $\overline{B} \to D\ell\overline{\nu}_\ell$ is given by

$$\frac{d\Gamma}{dw}(\overline{B} \to D\ell\overline{\nu}_\ell) =$$

$$\frac{G_F^2}{48\pi^3}|V_{cb}|^2(m_B + m_D)^2 m_D^3 (w^2-1)^{3/2}(\eta_{\rm em}\mathcal{G}(w))^2. \tag{11}$$

The form factor is

$$\mathcal{G}(w) = h_+(w) - \frac{m_B - m_D}{m_B + m_D} h_-(w), \tag{12}$$

where h_+ is normalized to unity in the infinite-mass limit due to HQS and h_- vanishes in the heavy-mass limit. Thus

$$\mathcal{G}(1) = 1 + \mathcal{O}\left(\frac{m_B - m_D}{m_B + m_D}\frac{1}{m_c}\right) \tag{13}$$

and the corrections to the HQET predictions are parametrically larger than was the case for $\overline{B} \to D^*\ell\overline{\nu}_\ell$.

In order to get a more precise prediction for the form factor $\mathcal{G}(1)$ the heavy-quark expansion can be supplemented by additional assumptions. It has been argued in Ref. [27] that in a limit in which the kinetic energy μ_π^2 is equal to the chromomagnetic moment μ_G^2 (these quantities are discussed below in more detail) one may obtain the value

$$\mathcal{G}(1) = 1.04 \pm 0.01_{\rm power} \pm 0.01_{\rm pert}. \tag{14}$$

Lattice calculations including effects beyond the heavy mass limit have become available, and hence the fact that deviations from the HQET predictions are parametrically larger than in the case $\overline{B} \to D^* \ell \overline{\nu}_\ell$ is irrelevant. These unquenched calculations quote a value (preliminary, from 2005) [28]

$$\mathcal{G}(1) = 1.074 \pm 0.018 \pm 0.016. \tag{15}$$

The measurements of $\overline{B} \to D \ell \overline{\nu}_\ell$ have improved substantially in the last few years. The new measurements [24,29] are consistent with previous measurements [17,30,31] but significantly more precise. The average of these inputs [26] gives $\mathcal{G}(1)|V_{cb}| = (42.6 \pm 0.7 \pm 1.4) \times 10^{-3}$. Using the value given in Eq. (15) for $\mathcal{G}(1)$, accounting for the electroweak correction and conservatively adding the theory uncertainties linearly results in

$$|V_{cb}| = (39.4 \pm 1.4 \pm 1.3) \times 10^{-3} \quad (\overline{B} \to D \ell \overline{\nu}_\ell, \text{ LQCD}), \tag{16}$$

where the first uncertainty is from experiment and the second from theory.

Using the non-lattice estimate from Eq. (14) one finds $|V_{cb}| = (40.7 \pm 1.5 \pm 0.8) \times 10^{-3}$.

Measuring the differential rate at $w = 1$ is more difficult in $\overline{B} \to D \ell \overline{\nu}_\ell$ decays than in $\overline{B} \to D^* \ell \overline{\nu}_\ell$ decays, since the rate is smaller and the background from mis-reconstructed $\overline{B} \to D^* \ell \overline{\nu}_\ell$ decays is significant; this is reflected in the larger experimental uncertainty. The B factories address these limitations by studying decays recoiling against fully reconstructed B mesons or doing a global fit to $\overline{B} \to X_c \ell \overline{\nu}_\ell$ decays. Theoretical input on the shape of the w spectrum in $\overline{B} \to D \ell \overline{\nu}_\ell$ is valuable, as precise measurements of the total rate are easier; recent measurements [24,29] of $\mathcal{B}(\overline{B} \to D \ell \overline{\nu}_\ell)$ have uncertainties of $\sim 5\%$.

The determinations from $\overline{B} \to D^* \ell \overline{\nu}_\ell$ and $\overline{B} \to D \ell \overline{\nu}_\ell$ decays are consistent, and their uncertainties are largely uncorrelated. Averaging these two lattice-based results gives

$$|V_{cb}| = (39.6 \pm 0.9) \times 10^{-3} \quad \text{(exclusive)}. \tag{17}$$

Prospects for Lattice determinations of the $B \to D^{(*)}$ form factors

Lattice determinations of the $B \to D^{(*)}$ form factors naturally build in heavy-quark symmetries, so all uncertainties scale with the deviation of the form factor from unity [32,33]. In combination with unquenched calculations, i.e. calculations with realistic sea quarks, one obtains quite precise calculations of the form factors, now at the 2% level. The dominant uncertainties are due to the chiral extrapolation from the light quark masses used in the numerical lattice computation to realistic up and down quark masses, and to discretization errors. These sources of uncertainty will be reduced with larger lattice sizes and smaller lattice spacings.

A further ongoing development is the extension of these calculations to nonzero recoil. Such calculations are especially helpful for avoiding the $w \to 1$ extrapolation in $B \to D$.

Decays to Excited D Meson States

Above the ground state D and D^* mesons lie four positive-parity states with one unit of orbital angular momentum, generically denoted as D^{**}. In the heavy mass limit they form two spin symmetry doublets with $j_\ell = 1/2$ and $j_\ell = 3/2$, where j_ℓ is the total angular momentum of the light degrees of freedom. The doublet with $j_\ell = 3/2$ is expected to be narrow while the states with $j_\ell = 1/2$ should be broad, consistent with experimental measurements. Furthermore, one expects that in the heavy mass limit $\Gamma(B \to D^{**}(j_\ell = 3/2)\ell\bar{\nu}) \gg \Gamma(B \to D^{**}(j_\ell = 1/2)\ell\bar{\nu})$ [34,35,36]. Measurements indicate that this expectation may be violated, although the experimental situation is not clear. BELLE [37] and BABAR [38] report different results for the broad states and the experiments do not have the sensitivity to identify the spin-parity of these states. It has been suggested that decays to radially excited charm mesons may play a role in this puzzle [39]. If a violation is confirmed, it may indicate substantial mixing between the two spin symmetry doublets, which can occur due to terms of order $1/m_c$. However, the impact on the exclusive $|V_{cb}|$ determination is expected to be small, since the zero-recoil point is protected against corrections of order $1/m_c$ by Luke's theorem.

$|V_{cb}|$ from inclusive decays

At present the most precise determinations of $|V_{cb}|$ come from inclusive decays. The method is based on a measurement of the total semileptonic decay rate, together with the leptonic energy and the hadronic invariant mass spectra of inclusive semileptonic decays. The total decay rate can be calculated quite reliably in terms of non-perturbative parameters that can be extracted from the information contained in the spectra.

Inclusive semileptonic rate

The theoretical foundation for the calculation of the total semileptonic rate is the Operator Product Expansion (OPE) which yields the Heavy Quark Expansion (HQE), a systematic expansion in inverse powers of the b-quark mass [40,41]. The validity of the OPE is proven in the deep Euclidean region for the momenta (which is satisfied, *e.g.*, in deep inelastic scattering), but its application to heavy-quark decays requires a continuation to time-like momenta $p_B^2 = M_B^2$, where possible contributions which are exponentially damped in the Euclidean region could become oscillatory. The validity of the OPE for inclusive decays is equivalent to the assumption of parton-hadron duality, hereafter referred to simply as duality, and possible oscillatory contributions would be an indication of duality violation.

Duality-violating effects are hard to quantify. In practice, they would appear as unnaturally large coefficents of higher order terms in the $1/m$ expansion [42]. The description of ~ 60 measurements in terms of ~ 6 free parameters in global fits to $\overline{B} \to X_c \ell \overline{\nu}_\ell$ decays provides a non-trivial testing ground for the HQE predictions. Present fits include terms up to order $1/m_b^3$, the coefficients of which have sizes as expected a priori by theory and are in quantitative agreement with extractions from other observables. The consistency of the data with these OPE fits will be discussed later; no indication is found that terms of order $1/m_b^4$ or higher are large, and there is no evidence for duality violations in the data. Thus duality or, likewise, the validity of the OPE, is assumed in the analysis, and no further uncertainty is assigned to potential duality violations.

The OPE result for the total rate can be written schematically (the details of the expression can be found, *e.g.*, in Ref. [43]) as

$$\begin{aligned}\Gamma =&|V_{cb}|^2\hat{\Gamma}_0 m_b^5(\mu)(1+A_{\rm ew})\times \\ &\left[z_0^{(0)}(r)+\frac{\alpha_s(\mu)}{\pi}z_0^{(1)}(r)+\left(\frac{\alpha_s(\mu)}{\pi}\right)^2 z_0^{(2)}(r)+\cdots\right. \\ &+\frac{\mu_\pi^2}{m_b^2}\left(z_2^{(0)}(r)+\frac{\alpha_s(\mu)}{\pi}z_2^{(1)}(r)+\cdots\right) \\ &+\frac{\mu_G^2}{m_b^2}\left(y_2^{(0)}(r)+\frac{\alpha_s(\mu)}{\pi}y_2^{(1)}(r)+\cdots\right) \\ &+\frac{\rho_{\rm D}^3}{m_b^3}\left(z_3^{(0)}(r)+\frac{\alpha_s(\mu)}{\pi}z_3^{(1)}(r)+\cdots\right) \\ &+\frac{\rho_{\rm LS}^3}{m_b^3}\left(y_3^{(0)}(r)+\frac{\alpha_s(\mu)}{\pi}y_3^{(1)}(r)+\cdots\right) \\ &\left.+z_4\left(r,\frac{s_i}{m_b^4},\frac{\alpha_s(\mu)}{\pi}\right)+...\right] \end{aligned} \tag{18}$$

where $A_{\rm ew}$ denotes the electroweak corrections, r is the ratio m_c/m_b and the y_i and z_i are known functions which appear in the perturbative expansion of the different orders of the heavy mass expansion. A similar expansion can be set up for moments of the distributions of charged-lepton energy, hadronic invariant mass and hadronic energy.

This expression is known up to order $1/m_b^5$, where the terms of order $1/m_b^n$ with $n>2$ have been computed only at tree level [44,45,46,47]. The leading term is the parton model, which is known completely to order α_s and α_s^2 [48–50], and the terms of order $\alpha_s^{n+1}\beta_0^n$ (where β_0 is the first coefficient of the QCD β function, $\beta_0=(33-2n_f)/3$) have been included by the usual BLM procedure [43,51,52]. Furthermore, the corrections of order $\alpha_s\mu_\pi^2/m_b^2$ have been computed [53].

Starting at order $1/m_b^3$ contributions with an infrared sensitivity to the charm mass m_c appear [46,54,112]. At order $1/m_b^3$ this "intrinsic charm" contribution is a $\log(m_c)$ in the coefficient of the Darwin term ρ_D^3. At higher orders, terms such as $1/m_b^3\times 1/m_c^2$ and $\alpha_s(m_c)1/m_b^3\times 1/m_c$ appear, which are comparable in size to the contributions of order $1/m_b^4$

The HQE parameters are given in terms of forward matrix elements; the parameters entering the expansion for orders up to $1/m_b^3$ are

$$\begin{aligned}
\overline{\Lambda} &= M_B - m_b\,, \\
\mu_\pi^2 &= -\langle B|\overline{b}(iD_\perp)^2 b|B\rangle\,, \\
\mu_G^2 &= \langle B|\overline{b}(iD_\perp^\mu)(iD_\perp^\nu)\sigma_{\mu\nu} b|B\rangle\,, \\
\rho_{\rm D}^3 &= \langle B|\overline{b}(iD_{\perp\mu})(ivD)(iD_\perp^\nu) b|B\rangle\,, \\
\rho_{\rm LS}^3 &= \langle B|\overline{b}(iD_\perp^\mu)(ivD)(iD_\perp^\nu)\sigma_{\mu\nu} b|B\rangle. \qquad (19)
\end{aligned}$$

The hadronic parameters of the orders $1/m_b^4$ and $1/m_b^5$ can be found in Ref. [47] while the five hadronic parameters s_i of the order $1/m_b^4$ can be found in Ref. [45]; these have not yet been included in the fits. The non-perturbative matrix elements depend on the renormalization scale μ, on the chosen renormalization scheme and on the quark mass m_b, and may eventually be calculated in Lattice QCD. The rates and the spectra depend strongly on m_b (or equivalently on $\overline{\Lambda}$), which makes the discussion of renormalization issues mandatory.

Using the pole mass definition for the heavy quark masses, it is well known that the corresponding perturbative series of decay rates does not converge very well, making a precision determination of $|V_{cb}|$ in such a scheme impossible. The solution to this problem is to choose an appropriate "short-distance" mass definition. Frequently used mass definitions are the kinetic scheme [14], or the 1S scheme [56]. Both of these schemes have been applied to semileptonic $b \to c$ transitions, yielding comparable results and uncertainties.

The 1S scheme eliminates the b quark pole mass by relating it to the perturbative expression for the mass of the 1S state of the Υ system. The physical mass of the $\Upsilon(1S)$ contains non-perturbative contributions, which have been estimated in Ref. [57]. These non-perturbative contributions are small; nevertheless, the best determination of the b quark mass in the 1S scheme is obtained from sum rules for $e^+e^- \to b\bar{b}$ [58].

Alternatively one may use a short-distance mass definition such as the $\overline{\rm MS}$ mass $m_b^{\overline{\rm MS}}(m_b)$. However, it has been argued that the scale m_b is unnaturally high for B decays, while

for smaller scales $\mu \sim 1\,\text{GeV}$ $m_b^{\overline{\text{MS}}}(\mu)$ is under poor control. For this reason the so-called "kinetic mass" $m_b^{\text{kin}}(\mu)$, has been proposed. It is the mass entering the non-relativistic expression for the kinetic energy of a heavy quark, and is defined using heavy-quark sum rules [14].

The HQE parameters also depend on the renormalization scale and scheme. The matrix elements given in Eq. (19) are defined with the full QCD fields and states, which is the definition frequently used in the kinetic scheme. Sometimes slightly different parameters λ_1 and λ_2 are used, which are defined in the infinite mass limit. The relation between these parameters is

$$\begin{aligned} \overline{\Lambda}_{\text{HQET}} &= \lim_{m_b\to\infty} \overline{\Lambda}\,, \quad & -\lambda_1 &= \lim_{m_b\to\infty} \mu_\pi^2\,, \\ \lambda_2 &= \lim_{m_b\to\infty} \mu_G^2\,, & \rho_1 &= \lim_{m_b\to\infty} \rho_D^3\,, \\ \rho_2 &= \lim_{m_b\to\infty} \rho_{LS}^3. \end{aligned} \tag{20}$$

Defining the kinetic energy and the chromomagnetic moment in the infinite-mass limit (as, *e.g.*, in the 1S scheme) requires that $1/m_b$ corrections to the matrix elements defined in Eq. (19) be taken into account once one goes beyond order $1/m_b^2$. As a result, additional quantities $\mathcal{T}_1 \cdots \mathcal{T}_4$ appear at order $1/m_b^3$. However, these quantities are correlated such that the total number of non-perturbative parameters to order $1/m_b^3$ is the same as in the scheme where m_b is kept finite in the matrix elements which define the non-perturbative parameters. A detailed discussion of these issues can be found in Ref. [59].

In order to define the HQE parameters properly one must adopt a renormalization scheme, as was done for the heavy quark mass. Since all these parameters can again be determined by heavy-quark sum rules, one may adopt a scheme similar to the kinetic scheme for the quark mass. The HQE parameters in the kinetic scheme depend on powers of the renormalization scale μ, and the above relations are valid in the limit $\mu \to 0$, leaving only logarithms of μ.

Some of these parameters also appear in the relation for the heavy hadron masses. The quantity $\overline{\Lambda}$ is determined once a definition is specified for the quark mass. The parameter

μ_G^2 can be extracted from the mass splitting in the lowest spin-symmetry doublet of heavy mesons [60]

$$\mu_G^2(\mu) = \frac{3}{4} C_G(\mu, m_b)(M_{B^*}^2 - M_B^2), \tag{21}$$

where $C_G(\mu, m_b)$ is a perturbatively-computable coefficient which depends on the scheme. In the kinetic scheme we have

$$\mu_G^2(1\text{GeV}) = 0.35^{+0.03}_{-0.02}\,\text{GeV}^2. \tag{22}$$

Determination of HQE Parameters and $|V_{cb}|$

Several experiments have measured moments in $\overline{B} \to X_c \ell \overline{\nu}_\ell$ decays [61–69] as a function of the minimum lepton momentum. The measurements of the moments of the electron energy spectrum (0^{th}-3^{rd}) and of the squared hadronic mass spectrum (0^{th}-2^{nd}) have statistical uncertainties that are roughly equal to their systematic uncertainties. They can be improved with more data and significant effort. The sets of moments measured by each experiment have strong correlations; the full statistical and systematic correlation matrices are required to allow these to be used in a global fit. Measurements of photon energy moments (0^{th}-2^{nd}) in $B \to X_s\gamma$ decays [70–74] as a function of the minimum accepted photon energy are still primarily statistics limited.

Global fits to the full set of moments [69,71,75–78] have been performed in the 1S and kinetic schemes. The semileptonic moments alone determine a linear combination of m_b and m_c very accurately but leave the orthogonal combination poorly determined [79]; additional input is required to allow a precise determination of m_b. This additional information can come from the radiative $B \to X_s\gamma$ moments, which provide complementary information on m_b and μ_π^2, or from precise determinations of the charm quark mass [80,81]. The values obtained in the kinetic scheme fits [77] with these two constraints are consistent. Based on the charm quark mass constraint [80], $m_c^{\overline{\text{MS}}}(3\,\text{GeV}) = 0.998 \pm 0.029\,\text{GeV}$,

$$|V_{cb}| = (41.88 \pm 0.44 \pm 0.59) \times 10^{-3} \tag{23}$$

$$m_b^{\text{kin}} = 4.560 \pm 0.023\,\text{GeV} \tag{24}$$

$$\mu_\pi^2(\text{kin}) = 0.453 \pm 0.036\,\text{GeV}^2, \tag{25}$$

where the first error on $|V_{cb}|$ includes experimental and theoretical uncertainties and the second error is from the estimated accuracy of the HQE for the total semileptonic rate.

Theoretical uncertainties are estimated and included in performing the fits. The χ^2/dof is substantially below unity in all fits, suggesting that the theoretical uncertainties may be overestimated. In any case, the low χ^2 shows no evidence for duality violations at a significant level. Similar values for the parameters are obtained when only experimental uncertainties are used in the fits. If the photon energy spectrum moments from $\overline{B} \to X_s\gamma$ are used in place of the constraint on the charm quark mass, the results change by only small amounts, e.g., $m_b^{\rm kin}$ increases to $4.574 \pm 0.032\,\mathrm{GeV}$. The mass in the $\overline{\rm MS}$ scheme corresponding to Eq. (24) is $m_b^{\overline{\rm MS}} = 4.19 \pm 0.04\,\mathrm{GeV}$, which can be compared with a recent value obtained using relativistic sum rules [82], $m_b^{\overline{\rm MS}} = 4.163 \pm 0.016\,\mathrm{GeV}$, and provides a non-trivial cross-check.

A fit to the same moments in the 1S scheme gives [78]

$$|V_{cb}| = (41.96 \pm 0.45 \pm 0.07) \times 10^{-3} \tag{26}$$

$$m_b^{\rm 1S} = 4.691 \pm 0.037\,\mathrm{GeV} \tag{27}$$

$$\lambda_1(\mathrm{1S}) = -0.362 \pm 0.067\,\mathrm{GeV}^2, \tag{28}$$

where the last error on $|V_{cb}|$ is due to the uncertainties in the B meson lifetimes. This fit uses semileptonic and radiative moments and constrains the chromomagnetic operator using the mass difference between the D and D^* mesons. This independent fit gives consistent results for $|V_{cb}|$ and, after translation to a common renormalization scheme, for m_b and μ_π^2.

The precision of the global fit results can be further improved. Some of the measurements, in particular of the $\overline{B} \to X_s\gamma$ photon energy spectrum, can be improved by using the full B-factory data sets. Improvements can be made in the theory by calculating higher order perturbative corrections to the coefficients of the HQE parameters, in particular the still missing $\alpha_s\mu_G^2$ corrections, which are presently only known for $B \to X_s\gamma$ [84]. The inclusion of still higher order moments may improve the sensitivity of the fits to higher order terms in the HQE.

Determination of $|V_{ub}|$

Summary: The determination of $|V_{ub}|$ is the focus of significant experimental and theoretical work. The determinations based on inclusive semileptonic decays using different calculational ansätze are consistent. The largest parametric uncertainty comes from the error on m_b. Significant progress has been made in determinations of $|V_{ub}|$ from $\overline{B} \to \pi \ell \overline{\nu}_\ell$ decays by using combined fits to theory and experimental data as a function of q^2. Further improvements in the form factor normalization are needed to improve the precision.

The values obtained from inclusive and exclusive determinations are

$$|V_{ub}| = (4.41 \pm 0.15 \,^{+\ 0.15}_{-\ 0.17}) \times 10^{-3} \quad \text{(inclusive)}, \tag{29}$$

$$|V_{ub}| = (3.23 \pm 0.31) \times 10^{-3} \quad \text{(exclusive)}. \tag{30}$$

The two determinations are independent, and the dominant uncertainties are on multiplicative factors. The inclusive and exclusive values are weighted by their relative errors and the uncertainties are treated as normally distributed. The resulting average has $p(\chi^2) = 0.01$, so we scale the error by $\sqrt{\chi^2/1} = 2.6$ to find

$$|V_{ub}| = (4.15 \pm 0.49) \times 10^{-3}. \tag{31}$$

Given the poor consistency between the two determinations, this average should be treated with caution.

$|V_{ub}|$ from inclusive decays

The theoretical description of inclusive $\overline{B} \to X_u \ell \overline{\nu}_\ell$ decays is based on the Heavy Quark Expansion, as for $\overline{B} \to X_c \ell \overline{\nu}_\ell$ decays, and leads to a predicted total decay rate with uncertainties below 5% [85,86]. Unfortunately, the total decay rate is hard to measure due to the large background from CKM-favored $\overline{B} \to X_c \ell \overline{\nu}_\ell$ transitions. Technically, the calculation of the partial decay rate in regions of phase space where $\overline{B} \to X_c \ell \overline{\nu}_\ell$ decays are suppressed is different from what has been described above, since it requires the introduction of a non-perturbative distribution function, the "shape function" (SF) [87,88]. Due to this, the theoretical input for the extraction on V_{ub} from inclusive decays is more challenging. The

shape function becomes important when the light-cone momentum component $P_+ \equiv E_X - |P_X|$ is not large compared to Λ_{QCD}. This additional difficulty can be addressed in two complementary ways. The leading shape function can either be measured in the radiative decay $\overline{B} \to X_s\gamma$, or be modeled with constraints on the $0^{\rm th}$-$2^{\rm nd}$ moments, and the results applied to the calculation of the $\overline{B} \to X_u\ell\overline{\nu}_\ell$ partial decay rate [89–91]; in such an approach the largest challenges are for the theory. Alternatively, measurements of $\overline{B} \to X_u\ell\overline{\nu}_\ell$ partial decay rates can be extended further into the $\overline{B} \to X_c\ell\overline{\nu}_\ell$-allowed region, enabling a simplified theoretical (pure HQE) treatment [92] but requiring precise experimental knowledge of the $\overline{B} \to X_c\ell\overline{\nu}_\ell$ background.

The shape function is a universal property of B mesons at leading order. It has been recognized for many years [87,88] that the leading SF can be measured in $\overline{B} \to X_s\gamma$ decays. However, sub-leading shape functions [93–98] arise at each order in $1/m_b$, and differ in semileptonic and radiative B decays. The form of the SFs cannot be calculated from first principles. Prescriptions that relate directly the partial rates for $\overline{B} \to X_s\gamma$ and $\overline{B} \to X_u\ell\overline{\nu}_\ell$ decays and thereby avoid any parameterization of the leading SF are available [99–102]; uncertainties due to sub-leading SFs remain in these approaches. Existing measurements have tended to use parameterizations of the leading SF that respect constraints on the zeroth, first and second moments. At leading order the first and second moments are equal to $\overline{\Lambda} = M_B - m_b$ and μ_π^2, respectively. The relations between SF moments and the non-perturbative parameters of the HQE are known to second order in α_s [103]. As a result, measurements of HQE parameters from global fits to $\overline{B} \to X_c\ell\overline{\nu}_\ell$ and $\overline{B} \to X_s\gamma$ moments can be used to constrain the SF moments, as well as provide accurate values of m_b and other parameters for use in determining $|V_{ub}|$. The possibility of measuring these HQE parameters directly from moments in $\overline{B} \to X_u\ell\overline{\nu}_\ell$ decays has been explored [104], but the experimental precision achievable there is not competitive with other approaches.

A recent development is to use appropriate basis functions to approximate the shape function, thereby also including the known short-distance contributions as well as the renormalization properties of the SF [105], in order to allow a global fit of all inclusive B meson decay data.

The calculations that are used for the fits performed by HFAG are documented in Refs. [89] (BLNP), [106] (GGOU), [107] (DGE) and [92] (BLL).

The calculations start from the triple diffential rate using the variables

$$P_l = M_B - 2E_l, \quad P_- = E_X + |\vec{P}_X|, \quad P_+ = E_X - |\vec{P}_X| \quad (32)$$

for which the differential rate becomes

$$\frac{d^3\Gamma}{dP_+\, dP_-\, dP_l} = \frac{G_F^2|V_{ub}|^2}{16\pi^2}(M_B - P_+) \quad (33)$$
$$\Big\{(P_- - P_l)(M_B - P_- + P_l - P_+)\mathcal{F}_1$$
$$+(M_B - P_-)(P_- - P_+)\mathcal{F}_2 + (P_- - P_l)(P_l - P_+)\mathcal{F}_3\Big\}.$$

The "structure functions" $\mathcal{F}_i$ can be calculated using factorization theorems that have been proven to subleading order in the $1/m_b$ expansion.

The BLNP [89] calculation uses these factorization theorems to write the $\mathcal{F}_i$ in terms of perturbatively calculable hard coefficients H and jet functions J, which are convolved with the (soft) light-cone distribution functions S, the shape functions of the B meson. The BLNP calculation has been updated to include the full $\mathcal{O}(\alpha_S^2)$ contributions [108].

The leading order term in the $1/m_b$ expansion of the $\mathcal{F}_i$ contains a single non-perturbative function and is calculated to subleading order in α_s, while at subleading order in the $1/m_b$ expansion there are several independent non-perturbative functions which have been calculated only at tree level in the α_s expansion.

To extract the non-perturbative input one can study the photon energy spectrum in $B \to X_s\gamma$ [91]. This spectrum is known at a similar accuracy as the P_+ spectrum in $B \to X_u\ell\overline{\nu}_\ell$. Going to subleading order in the $1/m_b$ expansion requires the

modeling of subleading SFs, a large variety of which were studied in Ref. [89].

A distinct approach (GGOU) [106] uses a hard, Wilsonian cut-off that matches the definition of the kinetic mass. The non-perturbative input is similar to what is used in BLNP, but the shape functions are defined differently. In particular, they are defined at finite m_b and depend on the light-cone component k_+ of the b quark momentum and on the momentum transfer q^2 to the leptons. These functions include sub-leading effects to all orders; as a result they are non-universal, with one shape function corresponding to each structure function in Eq. (33). Their k_+ moments can be computed in the OPE and related to observables and to the shape functions defined in Ref. [89].

Going to subleading order in α_s requires the definition of a renormalization scheme for the HQE parameters and for the SF. It has been noted that the relation between the moments of the SF and the forward matrix elements of local operators is plagued by ultraviolet problems which require additional renormalization. A possible scheme for improving this behavior has been suggested in Refs. [89,91], which introduce a particular definition of the quark mass (the so-called shape function scheme) based on the first moment of the measured spectrum. Likewise, the HQE parameters can be defined from measured moments of spectra, corresponding to moments of the SF.

One can also attempt to calculate the SF by using additional assumptions. One possible approach (DGE) is the so-called "dressed gluon exponentiation" [107], where the perturbative result is continued into the infrared regime using the renormalon structure obtained in the large β_0 limit, where β_0 has been defined following Eq. (18).

While attempts to quantify the SF are important, the impact of uncertainties in the SF is significantly reduced in some recent measurements that cover a larger portion of the $\overline{B} \to X_u \ell \overline{\nu}_\ell$ phase space. Several measurements using a combination of cuts on the leptonic momentum transfer q^2 and the hadronic invariant mass m_X as suggested in Ref. [109] have been made. Measurements of the electron spectrum in $\overline{B} \to X_u \ell \overline{\nu}_\ell$ decays have been made down to momenta of 1.9 GeV or even

lower, where SF uncertainties are not dominant. Of course, determining $\overline{B} \to X_u \ell \overline{\nu}_\ell$ partial rates in charm-dominated regions can bring in a strong dependence on the modeling of the $\overline{B} \to X_u \ell \overline{\nu}_\ell$ spectrum, which is problematic. The measurements quoted below have used a variety of functional forms to parameterize the leading SF; in no case does this lead to more than a 2% uncertainty on $|V_{ub}|$.

Weak Annihilation [110,111,106] (WA) can in principle contribute significantly in the restricted region (at high q^2) accepted by measurements of $\overline{B} \to X_u \ell \overline{\nu}_\ell$ decays. An estimate [92] based on leptonic D_s decays [111,112] leads to a $\sim 2\%$ uncertainty on the total $\overline{B} \to X_u \ell \overline{\nu}_\ell$ rate from the $\Upsilon(4S)$. The differential spectrum from WA decays is not well known, but they are expected to contribute predominantly at high q^2. More recent investigations of WA [112,113,114] confirm that WA is a small effect, but may become a significant source of uncertainty for $|V_{ub}|$ measurements that only accept a small fraction, f_u, of the full $\overline{B} \to X_u \ell \overline{\nu}_\ell$ phase space. Model-dependent limits on WA were determined in Ref. [115], where the CLEO data were fitted to combinations of WA models and a spectator $\overline{B} \to X_u \ell \overline{\nu}_\ell$ component and background. More direct experimental constraints [116] on WA have recently been made by comparing the $\overline{B} \to X_u \ell \overline{\nu}_\ell$ decay rates of charged and neutral B mesons. However, these constraints are not sensitive to the isoscalar contribution to WA. The sensitivity of $|V_{ub}|$ determinations to WA can also be reduced by removing the region at high q^2 in those measurements where q^2 is determined.

Measurements

We summarize the measurements used in the determination of $|V_{ub}|$ below. Given the improved precision and more rigorous theoretical interpretation of the recent measurements, earlier determinations [117–120] will not be further considered in this review.

Inclusive electron momentum measurements [121–123] reconstruct a single charged electron to determine a partial decay rate for $\overline{B} \to X_u \ell \overline{\nu}_\ell$ near the kinematic endpoint. This results

in a high $\mathcal{O}(50\%)$ selection efficiency and only modest sensitivity to the modeling of detector response. The decay rate can be cleanly extracted for $E_e > 2.3\,\mathrm{GeV}$, but this is deep in the SF region, where theoretical uncertainties are large. Measurements down to 2.0 or 1.9 GeV exist, but have low ($< 1/10$) signal-to-background (S/B) ratio, making the control of the $\overline{B} \to X_c \ell \overline{\nu}_\ell$ background a crucial point. In these analyses the inclusive electron momentum spectrum from $B\overline{B}$ events is determined by subtracting the $e^+e^- \to q\overline{q}$ continuum background using data samples collected just below $B\overline{B}$ threshold. The continuum-subtracted spectrum is fitted to a combination of a model $\overline{B} \to X_u \ell \overline{\nu}_\ell$ spectrum and several components ($D\ell\overline{\nu}_\ell$, $D^*\ell\overline{\nu}_\ell$, ...) of the $\overline{B} \to X_c \ell \overline{\nu}_\ell$ background. The resulting $|V_{ub}|$ values for various E_e cuts are given in Table 1. The leading uncertainty at the lower lepton momentum cuts comes from the $\overline{B} \to X_c \ell \overline{\nu}_\ell$ background. Prospects for reducing further the lepton momentum cut are improving in light of better knowledge of the semileptonic decays to higher mass $X_c \ell \overline{\nu}$ states [124,37]. The determination of $|V_{ub}|$ from these measurements is discussed below.

An untagged "neutrino reconstruction" measurement [125] from BABAR uses a combination [126] of a high-energy electron with a measurement of the missing momentum vector. This allows a much higher S/B$\sim$ 0.7 at the same E_e cut and a $\mathcal{O}(5\%)$ selection efficiency, but at the cost of a smaller accepted phase space for $\overline{B} \to X_u \ell \overline{\nu}_\ell$ decays and uncertainties associated with the determination of the missing momentum. A control sample of $\Upsilon(4S) \to B\overline{B}$ decays where one B is reconstructed as $\overline{B} \to D^0(X) e \overline{\nu}$ with $D^0 \to K^-\pi^+$ is used to reduce uncertainties from detector and background modeling. The corresponding values for $|V_{ub}|$ are given in Table 1.

The large samples accumulated at the B factories allow studies in which one B meson is fully reconstructed and the recoiling B decays semileptonically [127–130]. The experiments can fully reconstruct a "tag" B candidate in about 0.5% (0.3%) of B^+B^- ($B^0\overline{B}^0$) events. An electron or muon with center-of-mass momentum above 1.0 GeV is required amongst the charged tracks not assigned to the tag B and the remaining particles are

assigned to the X_u system. The full set of kinematic properties (E_ℓ, m_X, q^2, *etc.*) are available for studying the semileptonically decaying B, making possible selections that accept up to 70% of the full $\overline{B} \to X_u \ell \overline{\nu}_\ell$ rate. Despite requirements (e.g. on the square of the missing mass) aimed at rejecting events with additional missing particles, undetected or mis-measured particles from $\overline{B} \to X_c \ell \overline{\nu}_\ell$ decay (e.g., K_L^0 and additional neutrinos) remain an important source of uncertainty. Measurements with the largest kinematic acceptance (i.e. $E_\ell > 1\,\mathrm{GeV}$) lead to the smallest theoretical and overall uncertainties on $|V_{ub}|$.

BABAR [127] and BELLE [128,129] have measured partial rates with cuts on m_X, m_X and q^2, and P_+ based on large samples of $B\overline{B}$ events. Correlations amongst these related partial rates are taken into account in the average given in Table 1. In each case the experimental systematics have significant contributions from the modeling of $\overline{B} \to X_u \ell \overline{\nu}_\ell$ and $\overline{B} \to X_c \ell \overline{\nu}_\ell$ decays and from the detector response to charged particles, photons and neutral hadrons.

Determination of $|V_{ub}|$

The determination of $|V_{ub}|$ from the measured partial rates requires input from theory. The BLNP, GGOU and DGE calculations described previously are used to determine $|V_{ub}|$ from all measured partial $\overline{B} \to X_u \ell \overline{\nu}_\ell$ rates; the values [26] are given in Table 1. The m_b input values used are derived from the fitted value in equation Eq. (24): $m_b^{SF} = 4.588 \pm 0.025$ GeV for BLNP, $m_b^{\rm kin} = 4.560 \pm 0.023$ GeV for GGOU, and $m_b^{\overline{MS}} = 4.194 \pm 0.043$ GeV for DGE. The larger uncertainties on m_b^{SF} and $m_b^{\overline{MS}}$ reflect the effect of scheme translations, which are done at fixed-order in α_s.

As an illustration of the relative sizes of the uncertainties entering $|V_{ub}|$ we give the error breakdown for the GGOU average: statistical—2.0%; experimental—1.7%; $\overline{B} \to X_c \ell \overline{\nu}_\ell$ modeling—1.3%; $\overline{B} \to X_u \ell \overline{\nu}_\ell$ modeling—1.9%; HQE parameters —1.9%; higher-order corrections—1.4%; q^2 modeling—1.3%; Weak Annihilation—$^{+0}_{-1.9}$%; SF form—0.2%. The uncertainty on m_b dominates the uncertainty on $|V_{ub}|$ from HQE parameters, but no longer dominates the overall uncertainty.

The correlations amongst the multiple BABAR recoil-based measurements [127] are fully accounted for in the average. The statistical correlations amongst the other measurements used in the average are tiny (due to small overlaps among signal events and large differences in S/B ratios) and have been ignored. Correlated systematic and theoretical errors are taken into account, both within an experiment and between experiments.

Table 1: $|V_{ub}|$ (in units of 10^{-5}) from inclusive $\overline{B} \to X_u \ell \overline{\nu}_\ell$ measurements. The first uncertainty on $|V_{ub}|$ is experimental, while the second includes both theoretical and HQE parameter uncertainties. The values are listed in order of increasing f_u (0.19 to 0.90); those below the horizontal bar are based on recoil methods.

Ref.	cut	BLNP	GGOU	DGE
[121]	$E_e > 2.1$	$419 \pm 49 \,^{+\,26}_{-\,34}$	$393 \pm 46 \,^{+\,22}_{-\,29}$	$382 \pm 45 \,^{+\,23}_{-\,26}$
[125]	E_e-q^2	$466 \pm 31 \,^{+\,31}_{-\,36}$	not avail.	$432 \pm 29 \,^{+\,24}_{-\,29}$
[123]	$E_e > 2.0$	$448 \pm 25 \,^{+\,27}_{-\,28}$	$429 \pm 24 \,^{+\,18}_{-\,24}$	$428 \pm 24 \,^{+\,22}_{-\,24}$
[122]	$E_e > 1.9$	$488 \pm 45 \,^{+\,24}_{-\,27}$	$475 \pm 44 \,^{+\,17}_{-\,22}$	$479 \pm 44 \,^{+\,21}_{-\,24}$
[127]	m_X-q^2	$425 \pm 23 \,^{+\,23}_{-\,25}$	$417 \pm 22 \,^{+\,22}_{-\,25}$	$419 \pm 22 \,^{+\,18}_{-\,19}$
[127]	P_+	$402 \pm 25 \,^{+\,24}_{-\,23}$	$375 \pm 23 \,^{+\,30}_{-\,32}$	$410 \pm 25 \,^{+\,37}_{-\,28}$
[127]	m_X	$397 \pm 22 \pm 20$	$394 \pm 22 \,^{+\,16}_{-\,17}$	$416 \pm 23 \,^{+\,26}_{-\,22}$
[127]	$E_e > 1$	$428 \pm 24 \,^{+\,18}_{-\,20}$	$435 \pm 24 \,^{+\,9}_{-\,10}$	$440 \pm 24 \,^{+\,12}_{-\,13}$
[129]	$E_e > 1$	$447 \pm 27 \,^{+\,19}_{-\,21}$	$454 \pm 27 \,^{+\,10}_{-\,11}$	$460 \pm 27 \,^{+\,11}_{-\,13}$
		$440 \pm 15 \,^{+\,19}_{-\,21}$	$439 \pm 15 \,^{+\,12}_{-\,14}$	$445 \pm 15 \,^{+\,15}_{-\,16}$

The theoretical calculations produce very similar results for $|V_{ub}|$; the standard deviation of the theory predictions for the endpoint rate is 4.6%, for the m_X-q^2 rate is 2.2%, and for the $E_e > 1\,\text{GeV}$ rate is 0.8%. The $|V_{ub}|$ values do not show a marked trend versus the kinematic acceptance, f_u, for $\overline{B} \to X_u \ell \overline{\nu}_\ell$ decays. The p-values of the averages are in the range 30-50%, indicating that the ratios of calculated partial widths in the different phase space regions are in good agreement with ratios of measured partial branching fractions.

A recent calculation [108] at NNLO accuracy of the leading term in the partial rate for kinematically restrictive cuts (e.g.

near the electron endpoint energy) shows a surprisingly large change from the NLO calculation used in the BLNP method, increasing $|V_{ub}|$ by up to $\sim 8\%$ for some measurements. These updated calculations are not reflected in the BLNP values shown in Table 1. In the GGOU and the DGE approaches the inclusion of the dominant $\alpha_s^2\beta_0$ contributions do not suggest large α_s^2 corrections in these methods.

All calculations yield compatible $|V_{ub}|$ values and similar error estimates. We take the arithmetic mean of the values and errors to find

$$|V_{ub}| = (4.41 \pm 0.15_{\rm exp}\ ^{+0.15}_{-0.17\,\rm th}) \times 10^{-3} \quad \text{(inclusive)}. \qquad (34)$$

As was the case with $|V_{cb}|$, it is hard to assign an uncertainty to $|V_{ub}|$ for possible duality violations. However, theoretical arguments suggest that duality should hold even better in $b \to u\ell\overline{\nu}_\ell$ than in $b \to c\ell\overline{\nu}_\ell$ [42]. In any case, unless duality violations are much larger in $\overline{B} \to X_u\ell\overline{\nu}_\ell$ decays than in $\overline{B} \to X_c\ell\overline{\nu}_\ell$ decays, the precision of the $|V_{ub}|$ determination is not yet at the level where duality violations are likely to be significant.

Hadronization uncertainties also impact the $|V_{ub}|$ determination. The theoretical expressions are valid at the parton level and do not incorporate any resonant structure (*e.g.* $\overline{B} \to \pi\ell\overline{\nu}_\ell$); this must be added "by hand" to the simulated $\overline{B} \to X_u\ell\overline{\nu}_\ell$ event samples, since the detailed final state multiplicity and structure impacts the estimates of experimental acceptance and efficiency. The experiments have adopted procedures to input resonant structure while preserving the appropriate behavior in the kinematic variables averaged over the sample. The resultng uncertainties have been estimated to be $\sim$ 1-2% on $|V_{ub}|$.

A separate class of analyses follows the strategy discussed in Refs. [99–102], where integrals of differential distributions in $\overline{B} \to X_u\ell\overline{\nu}_\ell$ decays are compared with corresponding integrals in $\overline{B} \to X_s\gamma$ decays to extract $|V_{ub}|$, thereby eliminating the need to model the leading shape function. A study [132] using the measured BABAR electron spectrum in $\overline{B} \to X_u\ell\overline{\nu}_\ell$ decays

provides $|V_{ub}|$ determinations using all available "SF-free" calculations; the resulting $|V_{ub}|$ values have total uncertainties of $\sim 12\%$ and are compatible with the average quoted above.

The BLL [109] calculation can be used for measurements [128,130,131] with cuts on m_X and q^2. Using the same HQE parameter input as above yields a $|V_{ub}|$ value of $(4.62 \pm 0.20 \pm 0.29) \times 10^{-3}$, which is about 7% higher than the values obtained from the calculations used in Table 1 for these measurements.

Status and outlook

At present, as indicated by the average given above, the uncertainty on $|V_{ub}|$ from inclusive decays is at the 5% level. Are these uncertainties justified? The uncertainty on m_b was discussed in detail above. The uncertainties quoted in the calculations due to matching scales, higher order corrections, etc., are at the few percent level on $|V_{ub}|$. While these uncertainties are inherently difficult to quantify, the calculations take different approaches yet produce similar estimates. Experimental uncertainties have been assessed independently by BaBar and Belle. An important common source of uncertainty comes from modelling the $\overline{B} \to X_u \ell \overline{\nu}_\ell$ decays. Better measurements of these exclusive decays would be helpful in this regard, as would improved knowledge of the main $\overline{B} \to X_c \ell \overline{\nu}_\ell$ decays.

$|V_{ub}|$ from exclusive decays

Exclusive charmless semileptonic decays offer a complementary means of determining $|V_{ub}|$. For the experiments, the specification of the final state provides better background rejection, but the lower branching fraction reflects itself in lower yields compared with inclusive decays. For theory, the calculation of the form factors for $\overline{B} \to X_u \ell \overline{\nu}_\ell$ decays is challenging, but brings in a different set of uncertainties from those encountered in inclusive decays. In this review we focus on $\overline{B} \to \pi \ell \overline{\nu}_\ell$, as it is the most promising mode for both experiment and theory, and recent improvements have been made in both areas. Measurements of other exclusive states can be found in Refs. [135–140,154].

$\overline{B} \to \pi\ell\overline{\nu}_\ell$ form factor calculations The relevant form factors for the decay $\overline{B} \to \pi\ell\overline{\nu}_\ell$ are usually defined as

$$\langle\pi(p_\pi)|V^\mu|B(p_B)\rangle = \tag{35}$$
$$f_+(q^2)\left[p_B^\mu + p_\pi^\mu - \frac{m_B^2 - m_\pi^2}{q^2}q^\mu\right] + f_0(q^2)\frac{m_B^2 - m_\pi^2}{q^2}q^\mu$$

in terms of which the rate becomes (in the limit $m_\ell \to 0$)

$$\frac{d\Gamma}{dq^2} = \frac{G_F^2|V_{ub}|^2}{24\pi^3}|p_\pi|^3|f_+(q^2)|^2, \tag{36}$$

where p_π is the momentum of pion in the B meson rest frame.

Currently available non-perturbative methods for the calculation of the form factors include lattice QCD (LQCD) and light-cone sum rules (LCSR). The two methods are complementary in phase space, since the lattice calculation is restricted to the kinematical range of high momentum transfer q^2 to the leptons, to avoid large discretization errors, while light-cone sum rules provide information near $q^2 = 0$. Interpolations between these two regions can be constrained by unitarity and analyticity.

Unquenched simulations, for which quark loop effects in the QCD vacuum are fully incorporated, have become quite common, and the first results based on these simulations for the $\overline{B} \to \pi\ell\overline{\nu}_\ell$ form factors have been obtained by the Fermilab/MILC collaboration [141] and the HPQCD collaboration [142]. The two calculations differ in the way the b quark is simulated, with HPQCD using nonrelativistic QCD and Fermilab/MILC the so-called Fermilab heavy-quark method; they agree within the quoted errors.

In order to obtain the partially-integrated differential rate, the BK parameterization [143]

$$f_+(q^2) = \frac{c_B(1-\alpha_B)}{(1-\tilde{q}^2)(1-\alpha_B\tilde{q}^2)}, \tag{37}$$
$$f_0(q^2) = \frac{c_B(1-\alpha_B)}{(1-\tilde{q}^2/\beta_B)}, \tag{38}$$

with $\tilde{q}^2 \equiv q^2/m_{B^*}^2$ has been used frequently to extrapolate to small values of q^2. It includes the leading pole contribution

from B^*, and higher poles are modeled by a single pole. The heavy-quark scaling is satisfied if the parameters c_B, α_B and β_B scale appropriately. However, the BK parameterization should be used with some caution, since it is not consistent with SCET [144]. More recently, analyticity and unitarity bounds have been employed to constrain the form factors. Making use of the heavy-quark limit, stringent constraints on the shape of the form factor can be derived [144], and the conformal mapping of the kinematical variables onto the complex unit disc yields a rapidly converging series in this variable. The use of lattice data in combination with a data point at small q^2 from SCET or sum rules provides a stringent constraint on the shape of the form factor [145]. The form factor parametrization given in Ref. [145] has been applied to the extraction of $|V_{ub}|$ from $B \to \pi \ell \bar{\nu}_\ell$ using lattice data in Ref. [141].

Much work remains to be done, since the current combined statistical plus systematic errors in the lattice results are still at the $\sim 10\%$ level on $|V_{ub}|$ and need to be reduced. Reduction of errors to the $\sim$ 5-6% level for $|V_{ub}|$ will be feasible within the next few years, with the inclusion of numerical data at lighter pion masses and finer lattice spacings, as well as possibly two-loop or nonperturbative matching between lattice and continuum heavy-to-light current operators.

Another established non-perturbative approach to obtain the form factors is through Light-Cone QCD Sum Rules (LCSR), where the heavy mass limit has been discussed from the point of view of SCET in Ref. [147]. The sum-rule approach provides an approximation for the product $f_B f_+(q^2)$, valid in the region $0 < q^2 <\sim 12$ GeV^2. The determination of $f_+(q^2)$ itself requires knowledge of the decay constant f_B, which usually is obtained by replacing f_B by its two-point QCD (SVZ) sum rule [148] in terms of perturbative and condensate contributions. The advantage of this procedure is the approximate cancellation of various theoretical uncertainties in the ratio $(f_B f_+)/(f_B)$. The LCSR for $f_B f_+$ is based on the light-cone OPE of the relevant vacuum-to-pion correlation function, calculated in full QCD at finite b-quark mass. The resulting expressions actually comprise a triple expansion: in the twist t

of the operators near the light-cone, in α_s, and in the deviation of the pion distribution amplitudes from their asymptotic form, which is fixed from conformal symmetry.

There are multiple sources of uncertainties in the LCSR calculation, which are discussed in Refs. [149,150]. Currently, a total uncertainty slightly larger than 10% on $|V_{ub}|$ is extracted from a LCSR calculation of

$$\Delta\zeta(0, q^2_{max}) = \frac{G_F^2}{24\pi^3} \int_0^{q^2_{max}} dq^2\, p_\pi^3 |f_+(q^2)|^2$$
$$= \frac{1}{|V_{ub}|^2 \tau_{B_0}} \int_0^{q^2_{max}} dq^2\, \frac{d\mathcal{B}(B \to \pi\ell\nu)}{dq^2} \qquad (39)$$

which turn out to be [151]

$$\Delta\zeta(0, 12\,\mathrm{GeV}^2) = 4.59^{+1.00}_{-0.85}\,\mathrm{ps}^{-1}. \qquad (40)$$

It is interesting to note that the results from the LQCD and LCSR are consistent with each other when either the BK parameterization or parametrizations based on conformal mappings [145,146] are used to relate them. This increases confidence in the theoretical predictions for the rate of $\overline{B} \to \pi\ell\overline{\nu}_\ell$. This is complementary to the lattice results at large values of q^2, and the results from LCSR smoothly extrapolate the lattice data to small values of q^2.

An alternative determination of $|V_{ub}|$ has been proposed by several authors [152,153] based on a model-independent relation between rare decays such as $\overline{B} \to K^*\ell^+\ell^-$ and $\overline{B} \to \rho\ell\overline{\nu}_\ell$. However, it requires a precise measurement of the $\overline{B} \to K^*\ell^+\ell^-$ decay, which is a task for ultra-high-rate experiments.

$\overline{B} \to \pi\ell\overline{\nu}_\ell$ measurements

The $\overline{B} \to \pi\ell\overline{\nu}_\ell$ measurements fall into two broad classes: untagged, in which case the reconstruction of the missing momentum of the event serves as an estimator for the unseen neutrino, and tagged, in which the second B meson in the event is fully reconstructed in either a hadronic or semileptonic decay mode. The tagged measurements have high and uniform acceptance, S/B as high as 10, but low statistics. The untagged

measurements have somewhat higher background levels (S/B < 1) and make slightly more restrictive kinematic cuts, but have adequate statistics to measure the q^2 dependence of the form factor.

Table 2: Total and partial branching fractions for $\overline{B}^0 \to \pi^+\ell^-\overline{\nu}_\ell$, scaled to a common set of external inputs. The uncertainties are from statistics and systematics. Measurements of $\mathcal{B}(B^- \to \pi^0\ell^-\overline{\nu}_\ell)$ have been multiplied by a factor $2\tau_{B^0}/\tau_{B^+}$ to obtain the values below.

	$\mathcal{B}\times 10^4$	$\mathcal{B}(q^2 > 16) \times 10^4$
CLEO π^+, π^0 [139]	$1.38 \pm 0.15 \pm 0.11$	$0.41 \pm 0.08 \pm 0.04$
BABAR π^+, π^0 [140]	$1.41 \pm 0.05 \pm 0.08$	$0.32 \pm 0.02 \pm 0.03$
BABAR π^+ [154]	$1.42 \pm 0.05 \pm 0.07$	$0.33 \pm 0.03 \pm 0.03$
BELLE π^+, π^0 [155]	$1.49 \pm 0.04 \pm 0.07$	$0.40 \pm 0.02 \pm 0.02$
BELLE SL π^+ [156]	$1.42 \pm 0.19 \pm 0.15$	$0.37 \pm 0.10 \pm 0.04$
BELLE SL π^0 [156]	$1.41 \pm 0.26 \pm 0.15$	$0.36 \pm 0.15 \pm 0.04$
BELLE had π^+ [157]	$1.12 \pm 0.18 \pm 0.05$	$0.26 \pm 0.08 \pm 0.01$
BELLE had π^0 [157]	$1.22 \pm 0.22 \pm 0.05$	$0.41 \pm 0.11 \pm 0.02$
BABAR SL π^+ [158]	$1.39 \pm 0.21 \pm 0.08$	$0.46 \pm 0.13 \pm 0.03$
BABAR SL π^0 [158]	$1.78 \pm 0.28 \pm 0.15$	$0.44 \pm 0.17 \pm 0.06$
BABAR had π^+ [159]	$1.07 \pm 0.27 \pm 0.19$	$0.65 \pm 0.20 \pm 0.13$
BABAR had π^0 [159]	$1.52 \pm 0.41 \pm 0.30$	$0.48 \pm 0.22 \pm 0.12$
Average	$1.42 \pm 0.03 \pm 0.04$	$0.37 \pm 0.01 \pm 0.02$

CLEO has analyzed $\overline{B} \to \pi\ell\overline{\nu}_\ell$ and $\overline{B} \to \rho\ell\overline{\nu}_\ell$ using an untagged analysis [139]. Similar analyses have been done at BABAR [140,154] and BELLE [155]. The leading systematic uncertainties in the untagged $\overline{B} \to \pi\ell\overline{\nu}_\ell$ analyses are associated with modeling the missing momentum reconstruction, with backgrounds from $\overline{B} \to X_u\ell\overline{\nu}_\ell$ decays and $e^+e^- \to q\overline{q}$ continuum events, and with varying the form factor for the $\overline{B} \to \rho\ell\overline{\nu}_\ell$ decay. The values obtained for the full and partial branching fractions [26] are listed in Table 2 above the horizontal line. These BABAR and BELLE measurements provide the differential $\overline{B} \to \pi\ell\overline{\nu}_\ell$ rate versus q^2, shown in Fig. 2, which is used in the determination of $|V_{ub}|$ discussed below.

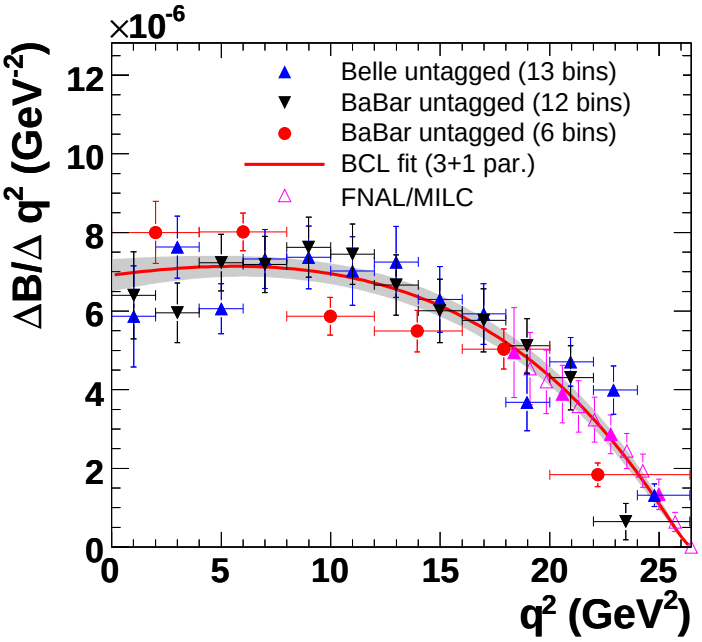

Figure 2: The untagged measurements of the differential $\overline{B} \to \pi\ell\overline{\nu}_\ell$ branching fraction versus q^2 that are used together with lattice calculations in the determination of $|V_{ub}|$.

Analyses [156,158] based on reconstructing a B in the $\overline{D}^{(*)}\ell^+\nu_\ell$ decay mode and looking for a $\overline{B} \to \pi\ell\overline{\nu}_\ell$ or $\overline{B} \to \rho\ell\overline{\nu}_\ell$ decay amongst the remaining particles in the event make use of the fact that the B and $\overline{B}$ are back-to-back in the $\Upsilon(4S)$ frame to construct a discriminant variable that provides a signal-to-noise ratio above unity for all q^2 bins. A related technique was discussed in Ref. [161]. BABAR [158] and BELLE [157] have also used their samples of B mesons reconstructed in hadronic decay modes to measure exclusive charmless semileptonic decays giving very clean but low-yield samples. The resulting full and partial branching fractions are given in Table 2. The averages take account of correlations and common systematic uncertainties, and have $p(\chi^2) > 0.5$ in each case.

$|V_{ub}|$ can be obtained from the average $\overline{B} \to \pi\ell\overline{\nu}_\ell$ branching fraction and the measured q^2 spectrum. Using the average [26] of partial branching fractions in the $q^2 < 12\,\mathrm{GeV}^2$ region,

$(0.81 \pm 0.02 \pm 0.03) \times 10^{-4}$, along with an LCSR calculation of the theoretical rate [151] gives

$$|V_{ub}| = (3.40 \pm 0.07_{\rm exp}{}^{+0.37}_{-0.32\ \rm theo}) \times 10^{-3} \quad (\text{LCSR}, q^2 < 12\,\text{GeV}^2). \tag{41}$$

Fits to the measured q^2 spectrum using a theoretically motivated parameterization (e.g. "BCL" from Ref. [146]) remove most of the model dependence from theoretical uncertainties in the shape of the spectrum. Recent determinations [26,141] of $|V_{ub}|$ from $\overline{B} \to \pi \ell \overline{\nu}_\ell$ decays have used simultaneous fits (see also Refs. [162]) to the experimental partial rate and lattice points versus q^2. A fit [26] to the untagged measurements incorporates the full statistical and systematic uncertainties in the measured spectrum and uses four lattice points in the region $q^2 > 16\,\text{GeV}^2$, taking into account their correlations. The fit, shown in Fig. 2, has $p(\chi^2) = 2.2\%$. If the tagged measurements, which are less consistent in the $q^2 < 8\,\text{GeV}^2$ region, are included, the fit gives $p(\chi^2) < 0.01\%$. We quote the result from the untagged measurements and add the difference (0.09×10^{-3}) between the $|V_{ub}|$ values from the two fits as an additional uncertainty to find

$$|V_{ub}| = (3.23 \pm 0.31\,) \times 10^{-3} \quad \text{(exclusive)}. \tag{42}$$

The largest contributions to the uncertainty come from lattice systematic and statistical errors, which will be further improved in the future.

Conclusion

The study of semileptonic B meson decays continues to be an active area for both theory and experiment. Substantial progress has been made in the application of HQE calculations to inclusive decays, where fits to moments of $\overline{B} \to X_c \ell \overline{\nu}_\ell$ decays provide precise values for $|V_{cb}|$ and, in conjunction with $B \to X_s \gamma$ decays or input on m_c, provide precise and consistent values for m_b. The values from the inclusive and exclusive $|V_{cb}|$ determinations are in reasonable agreement.

Continued improvements in measurements of inclusive $\overline{B} \to X_u \ell \overline{\nu}_\ell$ decays, along with additional theoretical studies of higher order contributions and improved knowledge of m_b,

have strengthened our determination of $|V_{ub}|$. Further progress in this area is possible, but will require better theoretical control over higher order terms, and improved experimental knowledge of the $\overline{B} \to X_c \ell \overline{\nu}_\ell$ background.

Progress in both $b \to u$ and $b \to c$ exclusive channels depends crucially on progress in lattice calculations. Here the prospects are good, since unquenched calculations are now available for the semileptonic form factors discussed here, as well as for other hadronic weak matrix elements needed to obtain the elements and phase of the CKM matrix [163,164]. Projections for future uncertainties from lattice calculations can be found in Ref. [165].

The measurements of the $\overline{B} \to \pi \ell \overline{\nu}_\ell$ branching fraction have uncertainties below 4%, and the measured q^2 dependence is reasonably precise. Reducing the theoretical uncertainties to a comparable level will require significant effort, but is clearly vital.

The difference between the values for $|V_{ub}|$ obtained from inclusive and exclusive decays has persisted for many years, despite significant improvements in both theory and experiment for both methods. How to reconcile these results remains an intriguing puzzle.

Both $|V_{cb}|$ and $|V_{ub}|$ are indispensable inputs into unitarity triangle fits. In particular, knowing $|V_{ub}|$ with good precision allows a test of CKM unitarity in the most direct way, by comparing the length of the $|V_{ub}|$ side of the unitarity triangle with the measurement of $\sin(2\beta)$. This comparison of a "tree" process ($b \to u$) with a "loop-induced" process ($B^0 - \overline{B}^0$ mixing) provides sensitivity to possible contributions from new physics. While the effort required to further improve our knowledge of these CKM matrix elements is large, it is well motivated.

The authors would like to acknowledge helpful input from C. Bozzi, J. Dingfelder, P. Gambino, A. Kronfeld, V. Luth, F. Muheim, C. Schwanda, P. Urquijo and R. Van de Water.

References

1. See R. Kowalewski and T. Mannel, J. Phys. **G37**, 075021 (2010).
2. E. Barberio *et al.*, `arXiv:0704.3575`.

3. N. Isgur and M.B. Wise, Phys. Lett. **B232**, 113 (1989); *ibid.* **B237**, 527 (1990).
4. M.A. Shifman and M.B. Voloshin, Sov. J. Nucl. Phys. **47**, 511 (1988) [Yad. Fiz. **47**, 801 (1988)].
5. M.E. Luke, Phys. Lett. **B252**, 447 (1990).
6. M. Ademollo and R. Gatto, Phys. Rev. Lett. **13**, 264 (1964).
7. A.V. Manohar and M.B. Wise, Camb. Monogr. Part. Phys. Nucl. Phys. Cosmol. **10**,1(2000).
8. B. Grinstein, Nucl. Phys. **B339**, 253 (1990); H. Georgi, Phys. Lett. **B240**, 447 (1990); A.F. Falk *et al.*, Nucl. Phys. **B343**, 1 (1990); E. Eichten and B. Hill, Phys. Lett. **B234**, 511 (1990).
9. C.G. Boyd, B. Grinstein, and R.F. Lebed, Phys. Rev. **D56**, 6895 (1997); *ibid.*, Phys. Rev. Lett. **74**, 4603 (1995); C.G. Boyd and M.J. Savage, Phys. Rev. **D56**, 303 (1997).
10. I. Caprini *et al.*, Nucl. Phys. **B530**, 153 (1998).
11. A. Sirlin, Nucl. Phys. **B196**, 83 (1982).
12. A. Czarnecki and K. Melnikov, Nucl. Phys. **B505**, 65 (1997).
13. Jon A. Bailey *et al.*, Fermilab Lattice and MILC collaborations, *Proceedings of Science LATTICE2010* (2010) 311. This is an update of C. Bernard *et al.*, Phys. Rev. **D79**, 014506 (2009).
14. I.I.Y. Bigi *et al.*, Phys. Rev. **D52**, 196 (1995).
15. A. Kapustin *et al.*, Phys. Lett. B **375**, 327 (1996).
16. P. Gambino, T. Mannel and N. Uraltsev, Phys. Rev. **D81**, 113002 (2010).
17. D. Buskulic *et al.*, (ALEPH Collab.), Phys. Lett. **B395**, 373 (1997).
18. G. Abbiendi *et al.*, (OPAL Collab.), Phys. Lett. **B482**, 15 (2000).
19. P. Abreu *et al.*, (DELPHI Collab.), Phys. Lett. **B510**, 55 (2001).
20. J. Abdallah *et al.*, (DELPHI Collab.), Eur. Phys. J. **C33**, 213 (2004).
21. N.E. Adam *et al.*, (CLEO Collab.), Phys. Rev. **D67**, 032001 (2003).
22. B. Aubert *et al.*, (BABAR Collab.), Phys. Rev. **D77**, 032002 (2008).
23. B. Aubert *et al.*, (BABAR Collab.), Phys. Rev. Lett. **100**, 231803 (2008).

24. B. Aubert *et al.*, (BABAR Collab.), Phys. Rev. **D79**, 012002 (2009).
25. W. Dungel *et al.*, (BELLE Collab.), Phys. Rev. **D82**, 112007 (2010).
26. `slac.stanford.edu/xorg/hfag2/semi/EndOfYear11/`.
27. N. Uraltsev, Phys. Lett. **B585**, 253 (2004).
28. M. Okamoto *et al.*, Nucl. Phys. (Proc. Supp.) **B140**, 461 (2005). A. Kronfeld, talk presented at the workshop CKM05, San Diego, CA - Workshop on the Unitarity Triangle, 15-18 March 2005.
29. B. Aubert *et al.*, (BABAR Collab.), Phys. Rev. Lett. **104**, 011802 (2010).
30. J. E. Bartelt *et al.*, (CLEO Collab.), Phys. Rev. Lett. **82**, 3746 (1999).
31. K. Abe *et al.*, (BELLE Collab.), Phys. Lett. **B526**, 247 (2002).
32. S. Hashimoto *et al.*, Phys. Rev. **D66**, 014503 (2002).
33. S. Hashimoto *et al.*, Phys. Rev. **D61**, 014502 (2000).
34. A.K. Leibovich *et al.*, Phys. Rev. D **57**, 308 (1998).
35. N. Uraltsev, `arXiv:hep-ph/0409125`.
36. I.I. Bigi *et al.*, Eur. Phys. J. C **52**, 975 (2007).
37. D. Liventsev *et al.*, (BELLE Collab.), Phys. Rev. **D77**, 091503 (2008).
38. B. Aubert *et al.*, (BABAR Collab.), Phys. Rev. Lett. **101**, 261802 (2008).
39. F. Bernlochner, Z. Ligeti, and S. Turczyk, `arXiv:1202.1834`.
40. A.V. Manohar and M.B. Wise, Phys. Rev. **D49**, 1310 (1994).
41. I.I.Y. Bigi *et al.*, Phys. Rev. Lett. **71**, 496 (1993), Phys. Lett. **B323**, 408 (1994).
42. M.A. Shifman, `hep-ph/0009131`, I.I.Y. Bigi and N. Uraltsev, Int. J. Mod. Phys. **A16**, 5201 (2001).
43. D. Benson *et al.*, Nucl. Phys. **B665**, 367 (2003).
44. M. Gremm and A. Kapustin, Phys. Rev. **D55**, 6924 (1997).
45. B. M. Dassinger, T. Mannel, and S. Turczyk, JHEP **0703**, 087 (2007).
46. I. I. Bigi, N. Uraltsev, and R. Zwicky, Eur. Phys. J. **C50**, 539 (2007).
47. T. Mannel, S. Turczyk, and N. Uraltsev, JHEP **1011**, 109 (2010).

48. A. Pak and A. Czarnecki, Phys. Rev. D **78**, 114015 (2008).
49. S. Biswas and K. Melnikov, JHEP **1002**, 089 (2010).
50. P. Gambino, JHEP **1109**, 055 (2011).
51. P. Gambino and N. Uraltsev, Eur. Phys. J. **C34**, 181 (2004).
52. V. Aquila *et al.*, Nucl. Phys. B **719**, 77 (2005).
53. T. Becher, H. Boos, and E. Lunghi, JHEP **0712**, 062 (2007).
54. C. Breidenbach *et al.*, Phys. Rev. D **78**, 014022 (2008).
55. I. Bigi *et al.*, `arXiv:0911.3322`.
56. A.H. Hoang *et al.*, Phys. Rev. **D59**, 074017 (1999).
57. H. Leutwyler, Phys. Lett. **B98**, 447 (1981);
    M.B. Voloshin, Sov. J. Nucl. Phys. **36**, 143 (1982).
58. A.H. Hoang, Phys. Rev. D **61**, 034005 (2000).
59. C.W. Bauer *et al.*, Phys. Rev. **D70**, 094017 (2004).
60. N. Uraltsev, Phys. Lett. B **545**, 337 (2002).
61. S.E. Csorna *et al.*, (CLEO Collab.), Phys. Rev. **D70**, 032002 (2004).
62. A.H. Mahmood *et al.*, (CLEO Collab.), Phys. Rev. **D70**, 032003 (2004).
63. B. Aubert *et al.*, (BABAR Collab.), Phys. Rev. **D69**, 111103 (2004).
64. B. Aubert *et al.*, (BABAR Collab.), Phys. Rev. **D69**, 111104 (2004).
65. C. Schwanda *et al.*, (BELLE Collab.), Phys. Rev. **D75**, 032005 (2007).
66. P. Urquijo *et al.*, (BELLE Collab.), Phys. Rev. **D75**, 032001 (2007).
67. J. Abdallah *et al.*, (DELPHI Collab.), Eur. Phys. J. **C45**, 35 (2006).
68. D. Acosta *et al.*, (CDF Collab.), Phys. Rev. **D71**, 051103 (2005).
69. B. Aubert *et al.*, (BABAR Collab.), Phys. Rev. **D81**, 032003 (2010).
70. A. Limosani *et al.* [BELLE Collab.], Phys. Rev. Lett. **103**, 241801 (2009).
71. C. Schwanda *et al.*, (BELLE Collab.), Phys. Rev. **D78**, 032016 (2008).
72. B. Aubert *et al.*, (BABAR Collab.), Phys. Rev. **D72**, 052004 (2005).

73. B. Aubert *et al.*, (BABAR Collab.), Phys. Rev. Lett. **97**, 171803 (2006).
74. S. Chen *et al.*, (CLEO Collab.), Phys. Rev. Lett. **87**, 251807 (2001).
75. M. Battaglia *et al.*, Phys. Lett. **B556**, 41 (2003).
76. B. Aubert *et al.*, (BABAR Collab.), Phys. Rev. Lett. **93**, 011803 (2004).
77. O. Buchmüller and H. Flächer, `hep-ph/0507253`; updated in Ref. [26].
78. C. W. Bauer *et al.*, Phys. Rev. **D70**, 094017 (2004); updated in Ref. [26].
79. See section 5.4.2 of M. Antonelli *et al.*, Phys. Reports **494**, 197 (2010).
80. B.Dehnadi, *et al.*, `arXiv:1102.2264`.
81. I. Allison *et al.*, (HPQCD Collab.), Phys. Rev. **D78**, 054513 (2008).
82. Chetyrkin *et al.*, Phys. Rev. **D80**, 074010 (2009).
83. M. Neubert, Phys. Rev. D **72**, 074025 (2005).
84. T. Ewerth, P. Gambino, and S. Nandi, Nucl. Phys. B **830**, 278 (2010).
85. A. H. Hoang *et al.*, Phys. Rev. **D59**, 074017 (1999).
86. N. Uraltsev, Int. J. Mod. Phys. **A14**, 4641 (1999).
87. M. Neubert, Phys. Rev. **D49**, 4623 (1994); *ibid.* **D49**, 3392 (1994).
88. I. Bigi *et al.*, Int. J. Mod. Phys. **A9**, 2467 (1994).
89. B.O. Lange, M. Neubert, and G. Paz, Phys. Rev. **D72**, 073006 (2005).
90. C. W. Bauer *et al.*, Phys. Lett. **B543**, 261 (2002).
91. T. Mannel and S. Recksiegel, Phys. Rev. **D60**, 114040 (1999).
92. C. W. Bauer, Z. Ligeti, and M. E. Luke, Phys. Rev. **D64**, 113004 (2001).
93. C. W. Bauer *et al.*, Phys. Rev. **D68**, 094001 (2003).
94. S. W. Bosch *et al.*, JHEP **0411**, 073 (2004).
95. A. W. Leibovich *et al.*, Phys. Lett. **B539**, 242 (2002).
96. M. Neubert, Phys. Lett. **B543**, 269 (2002).
97. K.S.M.Lee and I.W. Stewart, Nucl. Phys. **B721**, 325 (2005).
98. M. Beneke *et al.*, JHEP **0506**, 071 (2005).
99. M. Neubert, Phys. Lett. **B513**, 88 (2001); Phys. Lett. **B543**, 269 (2002).

100. A.K. Leibovich *et al.*, Phys. Rev. **D61**, 053006 (2000); **62**, 014010 (2000); Phys. Lett. **B486**, 86 (2000); **513**, 83 (2001).
101. A.H. Hoang *et al.*, Phys. Rev. **D71**, 093007 (2005).
102. B. Lange *et al.*, JHEP **0510**, 084 (2005); B. Lange, JHEP **0601**, 104 (2006).
103. M. Neubert, Phys. Lett. **B612**, 13 (2005).
104. P. Gambino, G. Ossola, and N. Uraltsev, JHEP **0509**, 010 (2005).
105. Z. Ligeti, I. W. Stewart, and F. J. Tackmann, Phys. Rev. D **78**, 114014 (2008).
106. P. Gambino *et al.*, JHEP **0710**, 058 (2007).
107. J.R. Andersen and E. Gardi, JHEP **0601**, 097 (2006).
108. C. Greub, M. Neubert, and B.D. Pecjak, Eur. Phys. J. C**65**, 501(2010).
109. C. W. Bauer *et al.*, Phys. Rev. **D64**, 113004 (2001); Phys. Lett. **B479**, 395 (2000).
110. I. I. Y. Bigi and N. G. Uraltsev, Nucl. Phys. **B423**, 33 (1994).
111. M.B. Voloshin, Phys. Lett. **B515**, 74 (2001).
112. I. Bigi, T. Mannel, S. Turczyk and N. Uraltsev, JHEP **1004**, 073 (2010).
113. Z. Ligeti, M. Luke, and A. V. Manohar, Phys. Rev. **D82**, 033003 (2010).
114. P. Gambino and J. F. Kamenik, Nucl. Phys. **B840**,424 (2010).
115. J.L. Rosner *et al.*, (CLEO Collab.), Phys. Rev. Lett. **96**, 121801 (2006).
116. B. Aubert *et al.*, (BABAR Collab.), `arXiv:0708.1753`.
117. R. Barate *et al.*, (ALEPH Collab.), Eur. Phys. J. **C6**, 555 (1999).
118. M. Acciarri *et al.*, (L3 Collab.), Phys. Lett. **B436**, 174 (1998).
119. G. Abbiendi *et al.*, (OPAL Collab.), Eur. Phys. J. **C21**, 399 (2001).
120. P. Abreu *et al.*, (DELPHI Collab.), Phys. Lett. **B478**, 14 (2000).
121. A. Bornheim *et al.*, (CLEO Collab.), Phys. Rev. Lett. **88**, 231803 (2002).
122. A. Limosani *et al.*, (BELLE Collab.), Phys. Lett. **B621**, 28 (2005).

123. B. Aubert *et al.*, (BABAR Collab.), Phys. Rev. **D73**, 012006 (2006).

124. B. Aubert *et al.*, (BABAR Collab.), Phys. Rev. **D76**, 051101 (2007); updated in `arXiv:0708.1738`.

125. B. Aubert *et al.*, (BABAR Collab.), Phys. Rev. Lett. **95**, 111801 (2005), Erratum-*ibid.* **97**, 019903(E) (2006).

126. R. Kowalewski and S. Menke, Phys. Lett. **B541**, 29 (2002).

127. J. P. Lees *et al.*, (BABAR Collab.), `arXiv:1112.0702`.

128. I. Bizjak *et al.*, (BELLE Collab.), Phys. Rev. Lett. **95**, 241801 (2005).

129. P. Urquijo *et al.*, (BELLE Collab.), Phys. Rev. Lett. **104**, 021801 (2010).

130. B. Aubert *et al.*, (BABAR Collab.), Phys. Rev. Lett. **96**, 221801 (2006).

131. H. Kakuno *et al.*, (BELLE Collab.), Phys. Rev. Lett. **92**, 101801 (2004).

132. V. Golubev, Y. Skovpen, and V. Luth, Phys. Rev. **D76**, 114003 (2007).

133. J.H. Kuhn, M. Steinhauser, and C. Sturm, Nucl. Phys. B **778**, 192 (2007).

134. I. Allison *et al.* [HPQCD Collab.], Phys. Rev. **D78**, 054513 (2008).

135. B. Aubert *et al.*, (BABAR Collab.), Phys. Rev. Lett. **90**, 181801 (2003).

136. T. Hokuue *et al.*, (BELLE Collab.), Phys. Lett. **B648**, 139 (2007).

137. B. Aubert *et al.*, (BABAR Collab.), Phys. Rev. **D79**, 052011 (2008).

138. C. Schwanda *et al.*, (BELLE Collab.), Phys. Rev. Lett. **93**, 131803 (2004).

139. N. E. Adam *et al.*, (CLEO Collab.), Phys. Rev. Lett. **99**, 041802 (2007); Phys. Rev. **D76**, 012007 (2007); supercedes Phys. Rev. **D68**, 072003 (2003).

140. P. del Amo Sanchez *et al.*, (BABAR Collab.), Phys. Rev. **D83**, 032007 (2011); supercedes B. Aubert *et al.*, (BABAR Collab.), Phys. Rev. **D72**, 051102 (2005).

141. J. Bailey *et al.*, (Fermilab/MILC), Phys. Rev. **D79**, 054507 (2009).

142. E. Dalgic *et al.*, (HPQCD), Phys. Rev. **D73**, 074502 (2006), Erratum-*ibid.* **D75** 119906 (2007).

143. D. Becirevic and A. B. Kaidalov, Phys. Lett. **B478**, 417 (2000).
144. T. Becher and R. J. Hill, Phys. Lett. **B633**, 61 (2006).
145. M. C. Arnesen *et al.*, Phys. Rev. Lett. **95**, 071802 (2005).
146. C. Bourrely, I. Caprini, and L. Lellouch, Phys. Rev. **D79**, 013008 (2009).
147. T. Hurth *et al.*, `hep-ph/0509167`.
148. M.A. Shifman, A.I. Vainshtein, and V.I. Zakharov, Nucl. Phys. **B147**, 385 (1979); *ibid.* **B147**, 448 (1979).
149. P. Ball and R. Zwicky, Phys. Rev. **D71**, 014015 (2005).
150. G. Duplancic *et al.*, JHEP **0804**, 014 (2008).
151. A. Khodjamirian *et al.*, Phys. Rev. **D83**, 094031 (2011).
152. N. Isgur and M.B. Wise, Phys. Rev. **D42**, 2388 (1990).
153. B. Grinstein and D. Pirjol, Phys. Rev. **D70**, 114005 (2004).
154. P. del Amo Sanchez *et al.*, (BABAR Collab.), Phys. Rev. **D83**, 052011 (2011).
155. H. Ha *et al.*, (BELLE Collab.), Phys. Rev. **D83**, 071101 (2011).
156. K. Abe *et al.*, (BELLE Collab.), Phys. Lett. **B648**, 139 (2007).
157. I. Adachi *et al.*, (BELLE Collab.), `arXiv:0812.1414`.
158. B. Aubert *et al.*, (BABAR Collab.), Phys. Rev. Lett. **101**, 081801 (2008).
159. B. Aubert *et al.*, (BABAR Collab.), Phys. Rev. Lett. **97**, 211801 (2006).
160. D. Scora and N. Isgur, Phys. Rev. **D52**, 2783 (1995).
161. W. Brower and H. Paar, Nucl. Instrum. Methods **A421**, 411 (1999).
162. P. Ball, `arXiv:0705.2290,`; J.M. Flynn and J. Nieves, Phys. Lett. **B649**, 269 (2007); T. Becher and R.J. Hill, Phys. Lett. **B633**, 61 (2006); M. Arnesen *et al.*, Phys. Rev. Lett. **95**, 071802 (2005).
163. J. Laiho, E. Lunghi, and R. S. Van de Water, Phys. Rev. D **81**, 034503 (2010) `[arXiv:0910.2928 [hep-ph]]`.
164. G. Colangelo, *et al.*, Eur. Phys. J. C **71**, 1695 (2011) `[arXiv:1011.4408 [hep-lat]]`.
165. USQCD Collab. (2011), `www.usqcd.org/documents/HiIntensityFlavor.pdf`.